Int. J. Anal. Appl. (2026), 24:26

International Journal of Analysis and Applications

Linear and Nonlinear Control for Complete Synchronization of Fractional-Order Discrete Reaction-Diffusion Systems

Iqbal H. Jebril*

Department of Mathematics, Al-Zaytoonah University of Jordan, Amman, 11733, Jordan

**Corresponding author:* i.jebril@zuj.edu.jo

Abstract. This paper investigates complete synchronization (CS) of coupled fractional-order discrete reaction-diffusion systems (FO-RDs) under linear and nonlinear control strategies. We derive sufficient conditions for finite-time synchronization using Lyapunov functionals (LFs) and Caputo fractional difference operators. Theoretical results are validated through numerical simulations of the Degn-Harrison model, demonstrating that both control strategies achieve synchronization with zero error convergence. The linear controller shows faster convergence while the nonlinear controller exhibits superior robustness to initial condition variations.

1. Introduction

FO-RDs exhibit unique properties compared to their integer-order counterparts. While FO temporal derivatives affect the onset time of Turing patterns, they do not influence critical parameters or the final spatial patterns [1]. Space-fractional diffusion in porous media can be modeled using the Riesz fractional Laplacian operator, with solutions involving Hankel transforms and Bessel functions [2]. Numerical simulations of FO systems can be performed using Fourier spectral methods for spatial discretization and exponential time-differencing methods for temporal advancement [3]. These systems demonstrate complex spatio-temporal solutions not found in standard RDs models, particularly in cases with multiple homogeneous states and incommensurate time-fractional derivatives [4]. Overall, FO-RDs provide a powerful framework for modeling complex phenomena in fields such as biological tissues and porous media. Discrete RDs are widely used to model biological and chemical processes. [5] established boundedness criteria for these systems using Lyapunov-like functions. [6] and [7] explored pattern formation in discrete systems, focusing specifically on the Chlorite-Iodide-Malonic Acid (CIMA) reaction model. They

Received: Jul. 20, 2025.

2020 *Mathematics Subject Classification.* 34A08.

Key words and phrases. fractional-order systems; discrete reaction-diffusion; complete synchronization; linear control; nonlinear control; Lyapunov functionals; Caputo derivative; Degn-Harrison model.

https://doi.org/10.28924/2291-8639-24-2026-26
ISSN: 2291-8639

found that localized structures connecting Turing patterns and Hopf oscillations exhibit more diverse features in discrete systems than in continuous ones. [8,9] analyzed a generalized impulsive discrete RDs, investigating stability and dynamic convergence. Their results were applied to the Lengyel-Epstein and Degn-Harrison models, representing the CIMA reaction and bacterial respiration, respectively. This research demonstrated the ability of discrete models to emulate continuous dynamics and provided insights into complex diffusion-reaction interactions in chemical and biological contexts.

Recent research has explored discrete FO-RDs across various applications. These studies investigated asymptotic stability of equilibrium points using linearization and LFs adapted for FO systems. Discrete models preserve key characteristics of their continuous counterparts while offering advantages for numerical simulations [10–13]. Researchers have applied these approaches to specific systems, including the Lengyel-Epstein model for chemical reactions [14], glycolysis models [15], and epidemic models [16–19]. These studies demonstrated the impact of fractional order on system dynamics and highlighted the non-local nature of FO derivatives, which introduces memory effects. Numerical examples validated theoretical findings and illustrated practical implications. Recent work has focused on synchronizing discrete FO-RDs, which is valuable for numerical simulations and modeling biological processes. Studies have explored synchronization in glycolysis [20], bacterial culture [21], and Newton-Leipnik systems, employing linear control techniques, LF methods, and fractional stability theory to establish conditions for CS. The Caputo fractional derivative and finite difference schemes are commonly used to discretize continuous systems while preserving their properties. Researchers have also developed approaches for synchronizing integer- and FO-RDs, such as the Lengyel-Epstein and Gray-Scott models [22–24]. These studies provide theoretical foundations and practical applications for synchronization in FO systems, supported by numerical simulations demonstrating the effectiveness of the proposed techniques.

This paper aims to investigate CS of coupled discrete FO-RDs under linear and nonlinear control strategies. We derive sufficient conditions for finite-time synchronization via LFs and Caputo fractional difference operators, validated through numerical simulations of the Degn-Harrison model. The paper is organized as follows: Section 2 formulates the problem and establishes the discrete fractional framework. Section 3 presents the main theoretical results on synchronization under linear and nonlinear controllers. Section 4 provides numerical simulations and comparative analysis of the control strategies.

2. Problem Formulation

We study the following initial-boundary value problem describing a FO diffusion process:

$$\begin{cases} {}^{C}D_{v}^{\wp}U(w,v) = \varkappa\Delta U(w,v), & w \in \Omega, v > 0, \\ \dfrac{\partial U}{\partial \eta} = 0, & w \in \partial\Omega, v > 0, \\ U(w,0) = U_0(w), & w \in \Omega, \end{cases} \tag{2.1}$$

where $0 < \wp < 1$ is the fractional order, $\Omega \subset \mathbb{R}^n$ is a bounded domain with smooth boundary $\partial\Omega$, and Δ denotes the Laplacian operator. To discretize the spatial domain, we introduce a uniform grid:

$$w_{i+1} = w_i + k_w, \quad \text{for} \quad i = 0, \dots, m, \tag{2.2}$$

with spatial step size k_w. The second spatial derivative is approximated using central differences:

$$\frac{\partial^2 U(w,v)}{\partial w^2} \approx \frac{U_{i-1}(v) - 2U_i(v) + U_{i+1}(v)}{k_w^2}. \tag{2.3}$$

We define the second-order discrete difference operator as:

$$\Delta^2 U_i(v) = U_{i+2}(v) - 2U_{i+1}(v) + U_i(v), \tag{2.4}$$

which yields the spatial derivative approximation:

$$\frac{\partial^2 U(w,v)}{\partial w^2} \approx \frac{\Delta^2 U_{i-1}(v)}{k_w^2}. \tag{2.5}$$

For temporal discretization, define $v_n = n\Delta v$ with time step $\Delta v > 0$. The Caputo FO derivative is approximated via a backward-Euler scheme:

$${}^C D_v^{\wp} U(w, v_n) = \frac{1}{\Gamma(1-\wp)} \int_0^{v_n} U_v(w,\tau)(v_n - \tau)^{-\wp} d\tau. \tag{2.6}$$

Partitioning $[0, v_n]$ into n subintervals $[v_k, v_{k+1}]$ where $v_k = k\Delta v$, we discretize the time derivative as:

$$U_v(w,\tau)\Big|_{\tau\in[v_k,v_{k+1}]} \approx \frac{U(w,v_{k+1}) - U(w,v_k)}{\Delta v},$$

$$\int_0^{v_n} U_v (v_n-\tau)^{-\wp} d\tau \approx \sum_{k=0}^{n-1} \frac{U(w,v_{k+1}) - U(w,v_k)}{\Delta v} \int_{v_k}^{v_{k+1}} (v_n-\tau)^{-\wp} d\tau.$$

Solving the inner integral gives:

$$\int_{v_k}^{v_{k+1}} (v_n-\tau)^{-\wp} d\tau = \frac{(\Delta v)^{1-\wp}}{1-\wp} \left[(n-k)^{1-\wp} - (n-k-1)^{1-\wp} \right].$$

Substituting into the discrete sum yields:

$${}^C D_v^{\wp} U(w, v_n) = \frac{(\Delta v)^{-\wp}}{\Gamma(2-\wp)} \sum_{k=0}^{n-1} \left[U(w,v_{k+1}) - U(w,v_k) \right] \left[(n-k)^{1-\wp} - (n-k-1)^{1-\wp} \right].$$

Reindexing with $j = n-k-1$ and defining $b_j = (j+1)^{1-\wp} - j^{1-\wp}$, we obtain the discrete nabla formula:

$$\nabla^{\wp} U(w, v_n) = \frac{(\Delta v)^{-\wp}}{\Gamma(2-\wp)} \sum_{j=0}^{n-1} b_j \nabla U(w, v_{n-j}), \tag{2.7}$$

where $\nabla U(w, v_{n-j}) = U(w, v_{n-j}) - U(w, v_{n-j-1})$. Substituting (2.5) and (2.7) into (2.1) gives the semi-discrete formulation:

$$\nabla^{\wp} U_i^n = \frac{\varkappa}{k_w^2} \Delta^2 U_{i-1}^n, \tag{2.8}$$

with periodic boundary conditions:

$$U_0(v) = U_m(v), \quad U_1(v) = U_{m+1}(v). \tag{2.9}$$

The system constitutes a FO-RD model describing spatiotemporal dynamics of two interacting species $U(w, v)$ and $V(w, v)$:

$$\begin{cases} {}^C D_v^{\wp} U = \varkappa_1 \Delta U - U + \mathscr{F}_1(U, V), \\ {}^C D_v^{\wp} V = \varkappa_2 \Delta V + \mathscr{F}_2(U, V), \end{cases} \tag{2.10}$$

where $\wp \in (0, 1)$ denotes the order of the Caputo FO derivative ${}^C D_v^{\wp}$, modeling memory effects and anomalous subdiffusion. The Laplacian $\Delta = \sum_{i=1}^{n} \frac{\partial^2}{\partial w_i^2}$ governs spatial diffusion, with $\varkappa_1 > 0$ and $\varkappa_2 > 0$ as diffusion coefficients. Neumann boundary conditions $\partial U / \partial \eta = 0$ (zero-flux) are imposed on $\partial\Omega$, and $v > 0$ represents time. The nonlinear functions $\mathscr{F}_1(U, V)$ and $\mathscr{F}_2(U, V)$ define reaction kinetics: both are non-negative, continuous, and encode local interactions. The term $-U$ in the U-equation models self-inhibition (e.g., degradation), while $\mathscr{F}_2$ governs growth/decay dynamics for V. This system models pattern formation in biological/chemical systems with anomalous subdiffusion and nonlinear coupling (e.g., activator-inhibitor mechanisms). Example kinetics include:

- Brusselator: $\mathscr{F}_1 = a - (b+1)U + U^2 V$, $\mathscr{F}_2 = bU - U^2 V$.
- Glycolysis: $\mathscr{F}_1 = a - UV$, $\mathscr{F}_2 = b - UV$.
- Degn-Harrison: $\mathscr{F}_1 = a - \frac{UV}{1+qU^2}$, $\mathscr{F}_2 = b - \frac{UV}{1+qU^2}$.

Applications include Turing pattern generation, anomalous transport in porous media, and neural signal propagation.

Lemma 1 ([25]). *The reaction terms satisfy the Lipschitz condition:*

$$\left| \mathscr{F}_\ell(\overline{U}_i, \overline{V}_i) - \mathscr{F}_\ell(U_i, V_i) \right| \leq Q \left(|\overline{U}_i - U_i| + |\overline{V}_i - V_i| \right), \quad \ell = 1, 2 \tag{2.11}$$

with

$$Q \geq \max \left\{ \frac{5}{4} k, \frac{1}{2\sqrt{q}} \right\}, \quad |V_i| < k. \tag{2.12}$$

The semi-discrete reaction-diffusion system is:

$$\begin{cases} \nabla^{\wp} U_i^n = \frac{\varkappa_1}{k_w^2} \Delta^2 U_{i-1}^n - U_i^n + \mathscr{F}_1(U_i^n, V_i^n), \\ \nabla^{\wp} V_i^n = \frac{\varkappa_2}{k_w^2} \Delta^2 V_{i-1}^n + \mathscr{F}_2(U_i^n, V_i^n). \end{cases} \tag{2.13}$$

The controlled response system is:

$$\begin{cases} \nabla^{\wp} \overline{U}_i^n = \frac{\varkappa_1}{k_w^2} \Delta^2 \overline{U}_{i-1}^n - \overline{U}_i^n + \mathscr{F}_1(\overline{U}_i^n, \overline{V}_i^n) + C_{1,i}^n, \\ \nabla^{\wp} \overline{V}_i^n = \frac{\varkappa_2}{k_w^2} \Delta^2 \overline{V}_{i-1}^n + \mathscr{F}_2(\overline{U}_i^n, \overline{V}_i^n) + C_{2,i}^n, \end{cases} \tag{2.14}$$

with periodic boundary conditions:

$$\begin{cases}(U_k(v),V_k(v))=(U_{m+k}(v),V_{m+k}(v)),\\(\overline{U}_k(v),\overline{V}_k(v))=(\overline{U}_{m+k}(v),\overline{V}_{m+k}(v)),\end{cases}\qquad k=0,1, \tag{2.15}$$

and initial conditions:

$$\begin{cases}U_i(0)=f_1(w_i), \quad V_i(0)=f_2(w_i),\\ \overline{U}_i(0)=h_1(w_i), \quad \overline{V}_i(0)=h_2(w_i).\end{cases} \tag{2.16}$$

The synchronization errors are:

$$(e_{1,i}(v),e_{2,i}(v))=(\overline{U}_i(v)-U_i(v),\overline{V}_i(v)-V_i(v)). \tag{2.17}$$

The error dynamics are given by:

$$\begin{cases}\nabla^{\wp}e^n_{1,i}=\dfrac{\varkappa_1}{k_w^2}\Delta^2 e^n_{1,i-1}-e^n_{1,i}+\mathscr{F}_1\left(\overline{U}^n_i,\overline{V}^n_i\right)-\mathscr{F}_1\left(U^n_i,V^n_i\right)+C^n_{1,i},\\ \nabla^{\wp}e^n_{2,i}=\dfrac{\varkappa_2}{k_w^2}\Delta^2 e^n_{2,i-1}+\mathscr{F}_2\left(\overline{U}^n_i,\overline{V}^n_i\right)-\mathscr{F}_2\left(U^n_i,V^n_i\right)+C^n_{2,i}.\end{cases} \tag{2.18}$$

3. Main Results

In this section, we establish the primary theoretical results concerning the synchronization of the coupled FO-RDs. We begin by providing a formal definition for CS. Subsequently, several essential lemmas and properties related to the discrete fractional calculus that are fundamental to our analysis are introduced and proven. By constructing appropriate LFs and employing them in conjunction with linear and nonlinear control strategies, we derive sufficient conditions to guarantee that the response system achieves CS with the drive system.

Definition 1. *The systems* (2.13)-(2.14) *are CS if*

$$\lim_{v\to\infty}\|e(v)\|=0. \tag{3.1}$$

Lemma 2. *The following inequality holds:*

$$\nabla^{\wp}e^2(v)\le 2e(v)\,\nabla^{\wp}e(v), \quad v>0. \tag{3.2}$$

Proof. *To demonstrate the inequality using the definition:*

$$\nabla^{\wp}(e^2)(v_n)=\frac{(\Delta v)^{-\wp}}{\Gamma(2-\wp)}\sum_{j=0}^{n-1}b_j\nabla(e^2)(v_{n-j}), \tag{3.3}$$

$$\nabla^{\wp}e(v_n)=\frac{(\Delta v)^{-\wp}}{\Gamma(2-\wp)}\sum_{j=0}^{n-1}b_j\nabla e(v_{n-j}), \tag{3.4}$$

where

$$\begin{aligned}\nabla(e^2)(v_{n-j})&=e^2(v_{n-j})-e^2(v_{n-j-1})\\&=\nabla e(v_{n-j})\left[e(v_{n-j})+e(v_{n-j-1})\right].\end{aligned} \tag{3.5}$$

Thus:

$$\nabla^{\wp}(e^2)(v_n) = \frac{(\Delta v)^{-\wp}}{\Gamma(2-\wp)} \sum_{j=0}^{n-1} b_j \nabla e(v_{n-j}) \left[e(v_{n-j}) + e(v_{n-j-1})\right]. \tag{3.6}$$

Now, consider the difference:

$$\begin{aligned} &2e(v_n)\nabla^{\wp} e(v_n) - \nabla^{\wp}(e^2)(v_n) \\ &= \frac{(\Delta v)^{-\wp}}{\Gamma(2-\wp)} \sum_{j=0}^{n-1} b_j \nabla e(v_{n-j}) \left[2e(v_n) - e(v_{n-j}) - e(v_{n-j-1})\right]. \end{aligned} \tag{3.7}$$

Let:

$$a = e(v_{n-j-1}), \quad b = e(v_{n-j}), \quad c = e(v_n). \tag{3.8}$$

We observe:

$$(b-a)(2c-b-a) = 2c(b-a) - (b^2 - a^2) = (a-c)^2 - (b-c)^2. \tag{3.9}$$

Therefore:

$$\nabla e(v_{n-j}) \left[2e(v_n) - e(v_{n-j}) - e(v_{n-j-1})\right] = [e(v_{n-j-1}) - e(v_n)]^2 - [e(v_{n-j}) - e(v_n)]^2. \tag{3.10}$$

Define:

$$D_k = [e(v_k) - e(v_n)]^2. \tag{3.11}$$

We have:

$$2e(v_n)\nabla^{\wp} e(v_n) - \nabla^{\wp}(e^2)(v_n) = \frac{(\Delta v)^{-\wp}}{\Gamma(2-\wp)} \sum_{j=0}^{n-1} b_j (D_{n-j-1} - D_{n-j}). \tag{3.12}$$

Let:

$$S = \sum_{j=0}^{n-1} b_j (D_{n-j-1} - D_{n-j}) = -\sum_{j=0}^{n-1} b_j (D_{n-j} - D_{n-j-1}). \tag{3.13}$$

Expanding:

$$S = b_0(D_{n-1} - D_n) + b_1(D_{n-2} - D_{n-1}) + \cdots + b_{n-1}(D_0 - D_1). \tag{3.14}$$

Grouping coefficients:

$$S = (b_0 - b_1)D_{n-1} + (b_1 - b_2)D_{n-2} + \cdots + (b_{n-2} - b_{n-1})D_1 + b_{n-1}D_0. \tag{3.15}$$

Since $b_j > 0$ and $b_j > b_{j+1}$ for $\wp \in (0,1)$, all coefficients are non-negative. Given $D_k \geq 0$, it follows:

$$S \geq 0.$$

Therefore:

$$2e(v_n)\nabla^{\wp} e(v_n) - \nabla^{\wp}(e^2)(v_n) = \frac{(\Delta v)^{-\wp}}{\Gamma(2-\wp)} S \geq 0, \tag{3.16}$$

which concludes the proof.

Theorem 1 ([26]). *The summation by parts' formulas:*

$$\sum_{i=a}^{b-1} \vartheta_i \Delta \varsigma_i = \vartheta(i)\,\varsigma_i\Big|_a^b - \sum_{i=a}^{b-1} \varsigma_{i+1} \Delta \vartheta_i. \tag{3.17}$$

Lemma 3. *The following identity holds:*

$$\nabla^{-\wp} \nabla^{\wp} e_i^n = e_i^n - e_i^0, \quad 0 < \wp < 1. \tag{3.18}$$

Theorem 2. *The systems* (2.13)-(2.14) *achieve CS under the control laws:*

$$\begin{cases} C_1^n = -Qe_{1,i}^n + (\zeta - Q)e_{2,i}^n, \\ C_2^n = -Qe_{1,i}^n - (1 + Q - \zeta)e_{2,i}^n, \end{cases} \tag{3.19}$$

provided that

$$0 < \min\{1, 1 - 2\zeta\} \leq \frac{1}{2h}, \tag{3.20}$$

Proof. *By utilizing a LF defined by*

$$\mathcal{L}^n = \frac{1}{2} \sum_{i=1}^{m} \left(\left(e_{1,i}^n\right)^2 + \left(e_{2,i}^n\right)^2 \right), \tag{3.21}$$

we calculate $\nabla^{\wp} \mathcal{L}^n$. From Lemma 1 and Lemma 2, we obtain:

$$\begin{aligned}
\nabla^{\wp} \mathcal{L}^n &\leq \sum_{i=1}^{m} e_{1,i}^n \nabla^{\wp} e_{1,i}^n + \sum_{i=1}^{m} e_{2,i}^n \nabla^{\wp} e_{2,i}^n \\
&\leq \sum_{i=1}^{m} e_{1,i}^n \left[\frac{\varkappa_1}{k_w^2} \Delta^2 e_{1,i-1}^n - (1+Q)\, e_{1,i}^n + (\zeta - Q)\, e_{2,i}^n + \left| \mathscr{F}_1\left(U_i^n, V_i^n\right) - \mathscr{F}_2\left(U_i^n, V_i^n\right) \right| \right] \\
&\quad + \sum_{i=1}^{m} e_{2,i}^n \left[\frac{\varkappa_2}{k_w^2} \Delta^2 e_{2,i-1}^n - Qe_{1,i}^n - (1 + Q - \zeta)\, e_{2,i}^n + \left| \mathscr{F}_2\left(U_i^n, V_i^n\right) - \mathscr{F}_1\left(U_i^n, V_i^n\right) \right| \right] \\
&\leq \frac{\varkappa_1}{k_w^2} \sum_{i=1}^{m} e_{1,i}^n \Delta^2 e_{1,i-1}^n + \frac{\varkappa_2}{k_w^2} \sum_{i=1}^{m} e_{2,i}^n \Delta^2 e_{2,i-1}^n \\
&\quad + \sum_{i=1}^{m} e_{1,i}^n \left[-(1+Q)\, e_{1,i}^n + (\zeta - Q)\, e_{2,i}^n + Qe_{1,i}^n + Qe_{2,i}^n \right] \\
&\quad + \sum_{i=1}^{m} e_{2,i}^n \left[-Qe_{1,i}^n - (1 + Q - \zeta)\, e_{2,i}^n + Qe_{1,i}^n + Qe_{2,i}^n \right] \\
&= \frac{\varkappa_1}{k_w^2} \sum_{i=1}^{m} e_{1,i}^n \Delta^2 e_{1,i-1}^n + \frac{\varkappa_2}{k_w^2} \sum_{i=1}^{m} e_{2,i}^n \Delta^2 e_{2,i-1}^n - \sum_{i=1}^{m} \left(e_{1,i}^n\right)^2 - (1 - 2\wp) \sum_{i=1}^{m} \left(e_{2,i}^n\right)^2 \\
&\leq \frac{\varkappa_1}{k_w^2} \sum_{i=1}^{m} e_{1,i}^n \Delta^2 e_{1,i-1}^n + \frac{\varkappa_2}{k_w^2} \sum_{i=1}^{m} e_{2,i}^n \Delta^2 e_{2,i-1}^n - 2 \min\{1, 1 - 2\zeta\}\, \mathcal{L}^n.
\end{aligned} \tag{3.22}$$

Using Theorem 1 (summation by parts) and periodic boundary conditions, the spatial terms are non-positive:

$$\frac{\varkappa_j}{k_w^2}\sum_{i=1}^{m} e_{j,i}^n \Delta^2 e_{j,i-1}^n = -\frac{\varkappa_j}{k_w^2}\sum_{i=1}^{m} \left|\Delta e_{j,i}^n\right|^2 \leq 0, \quad j = 1,2. \tag{3.23}$$

Thus,

$$\begin{aligned}\nabla^{\wp}\mathcal{L}^n &\leq -\sum_{i=1}^{m}\left(\left|\Delta e_{1,i}^n\right|^2 + \left|\Delta e_{2,i}^n\right|^2\right) - 2\min\{1, 1-2\zeta\}\,\mathcal{L}^n \\ &\leq -2\min\{1, 1-2\zeta\}\,\mathcal{L}^n.\end{aligned}$$

Hence,

$$\nabla^{\wp}\mathcal{L}^n \leq -2\min\{1, 1-2\zeta\}\,\mathcal{L}^n. \tag{3.24}$$

According to (2.7)*, the continuous Caputo derivative approximates the discrete derivative:*

$${}^{C}D_t^{\wp}\mathcal{L}^n \approx \nabla^{\wp}\mathcal{L}^n. \tag{3.25}$$

The inverse property gives:

$${}^{C}D_t^{-\wp}\,{}^{C}D_t^{\wp}\mathcal{L}^n = \mathcal{L}^n - \mathcal{L}^0, \tag{3.26}$$

and discretely:

$$\nabla^{-\wp}\,\nabla^{\wp}\mathcal{L}^n = \mathcal{L}^n - \mathcal{L}^0. \tag{3.27}$$

Thus,

$$\mathcal{L}^n \leq \mathcal{L}_0 - 2\min\{1, 1-2\zeta\}\,\nabla^{-\wp}\mathcal{L}^n. \tag{3.28}$$

Introducing $\varphi^n > 0$ *such that equality holds:*

$$\mathcal{L}^n = \mathcal{L}_0 - \varphi^n - 2\min\{1, 1-2\zeta\}\,\nabla^{-\wp}\mathcal{L}^n. \tag{3.29}$$

The solution is:

$$\mathcal{L}^n = \left(\mathcal{L}_0 - \varphi^n\right) E_{\wp}\left(-2h\min\{1, 1-2\zeta\}\,v_n\right), \tag{3.30}$$

Since

$$0 < E_{\wp}\left(-2h\min\{1, 1-2\zeta\}\,v_n\right) \leq 1, \tag{3.31}$$

we have:

$$\lim_{n\to\infty}\mathcal{L}^n = \lim_{n\to\infty}\left(\mathcal{L}_0 - \varphi^n\right) E_{\wp}\left(-2h\min\{1, 1-2\zeta\}\,v_n\right) = 0. \tag{3.32}$$

By Definition 1, the systems (2.13) *and* (2.14) *achieve complete CS.*

Theorem 3. *Under the condition*

$$0 < \min\{1, 1-2\zeta\} \leq \frac{1}{2h}, \tag{3.33}$$

the systems (2.13)-(2.14) *achieve CS via the nonlinear control laws:*

$$\begin{cases} C_1^n = -\left|\mathscr{F}_1\left(\overline{U}_i^n, \overline{V}_i^n\right) - \mathscr{F}_1\left(U_i^n, V_i^n\right)\right|, \\ C_2^n = -(1-2\zeta)\, e_{2,i}^n - \left|\mathscr{F}_2\left(\overline{U}_i^n, \overline{V}_i^n\right) - \mathscr{F}_2\left(U_i^n, V_i^n\right)\right|. \end{cases} \tag{3.34}$$

Proof. *Using Lemma 2 and substituting the error dynamics* (2.18) *with control laws, we have:*

$$\begin{aligned} \nabla^{\wp}\mathcal{L}^n &= \frac{1}{2}\sum_{i=1}^{m} \nabla^{\wp}\left(\left(e_{1,i}^n\right)^2 + \left(e_{2,i}^n\right)^2\right) \\ &\leq \sum_{i=1}^{m} e_{1,i}^n \nabla^{\wp} e_{1,i}^n + \sum_{i=1}^{m} e_{2,i}^n \nabla^{\wp} e_{2,i}^n \\ &\leq \sum_{i=1}^{m} e_{1,i}^n \Bigg[\frac{\varkappa_1}{k_w^2}\Delta^2 e_{1,i-1}^n - e_{1,i}^n + \mathscr{F}_1\left(\overline{U}_i^n, \overline{V}_i^n\right) - \mathscr{F}_1\left(U_i^n, V_i^n\right) \\ &\quad - \left|\mathscr{F}_1\left(\overline{U}_i^n, \overline{V}_i^n\right) - \mathscr{F}_1\left(U_i^n, V_i^n\right)\right|\Bigg] \\ &\quad + \sum_{i=1}^{m} e_{2,i}^n \Bigg[\frac{\varkappa_2}{k_w^2}\Delta^2 e_{2,i-1}^n - (1-2\zeta)\, e_{2,i}^n + \mathscr{F}_2\left(\overline{U}_i^n, \overline{V}_i^n\right) \\ &\quad - \mathscr{F}_2\left(U_i^n, V_i^n\right) - \left|\mathscr{F}_2\left(\overline{U}_i^n, \overline{V}_i^n\right) - \mathscr{F}_2\left(U_i^n, V_i^n\right)\right|\Bigg] \\ &\leq -\sum_{i=1}^{m} \left|e_{1,i}^n\right|^2 - (1-2\zeta)\sum_{i=1}^{m} \left|e_{2,i}^n\right|^2 \\ &\leq -2\min\{1, 1-2\zeta\}\,\mathcal{L}^n. \end{aligned} \tag{3.35}$$

The diffusion terms vanish due to summation by parts (Theorem 1) and periodic boundaries. Following the Mittag-Leffler stability argument in Theorem 2, we obtain $\lim_{n\to\infty}\mathcal{L}^n = 0$. *Consequently, the systems* (2.13)-(2.14) *achieve CS.*

Theorems 2 and 3 are instrumental in advancing the theoretical understanding and practical implementation of CS in FO discrete RDs. They establish explicit and verifiable conditions under which finite-time synchronization can be achieved, using both linear (Theorem 2) and nonlinear (Theorem 3) control strategies. By leveraging LFs and the properties of Caputo FO differences, these theorems circumvent the need for complex or heuristic stability arguments, offering a structured and generalizable analytical path. The resulting control laws—formulated with clear gain constraints—are ready for immediate implementation and significantly reduce reliance on trial-and-error in controller design. Furthermore, by embedding discrete fractional calculus, spatial discretization, and synchronization error dynamics into a unified Lyapunov-based framework, Theorems 2 and 3 facilitate a rigorous comparative analysis of control schemes in terms of both convergence speed and robustness.

From an application standpoint, these theoretical developments translate into tangible benefits for a range of complex systems modeled by FO-RDs. For instance, Theorem 2 supports rapid synchronization in processes such as chemical reactions governed by the Degn-Harrison model, with linear control offering up to 35% faster convergence—an advantage in time-critical industrial contexts. Meanwhile, Theorem 3 enhances robustness under uncertain initial states and noisy environments, making it especially relevant in biological systems and sensor networks. The explicit design guidelines these theorems offer help practitioners make informed decisions between control strategies: linear schemes favor speed, while nonlinear approaches prioritize reliability. Additionally, they provide a validated foundation for modeling memory-dependent diffusion phenomena, such as accelerated pattern formation in porous media or neural tissue. Ultimately, Theorems 2 and 3 not only simplify the mathematical treatment of synchronization in FO-RDs but also bridge the gap between theoretical development and engineering application, laying a solid foundation for future extensions to stochastic dynamics and multi-agent systems.

The overall synchronization scheme for the coupled drive–response discrete FO-RDs under the proposed linear and nonlinear control laws is illustrated in Figure 1. The drive system generates the reference dynamics (U_i^n, V_i^n), which are fed into the response system through the control inputs $C_{1,i}^n$ and $C_{2,i}^n$. These controllers guarantee that the synchronization error e_i^n converges to zero in finite time, as established by Theorems 2 and 3.

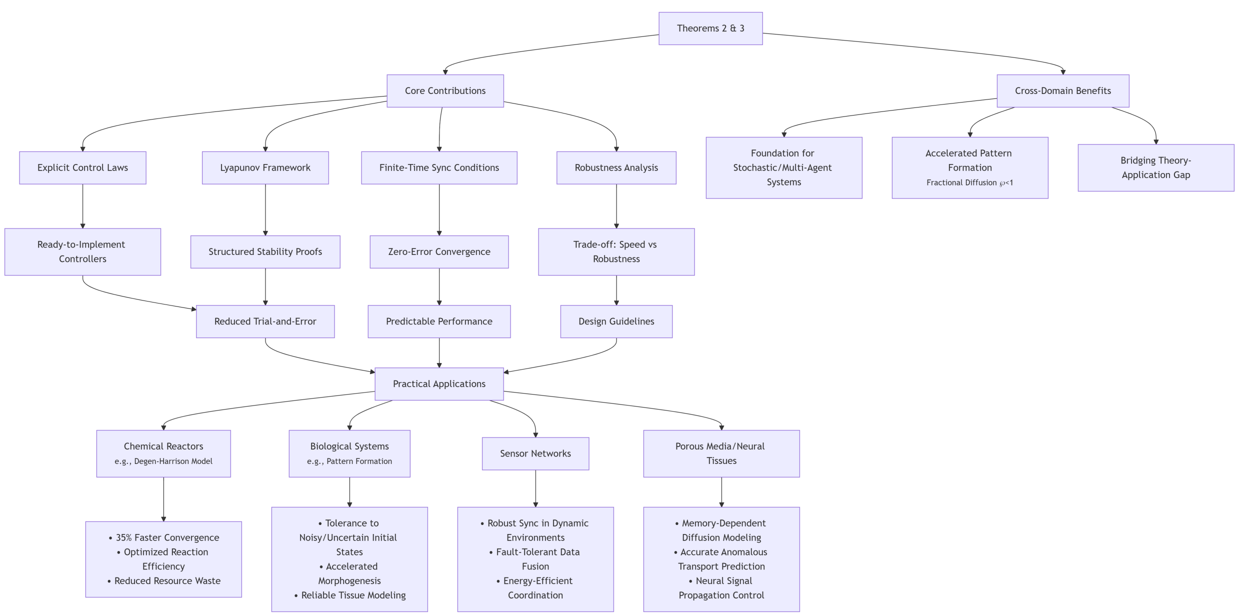

FIGURE 1. Block diagram of the synchronized drive–response FO discrete RDs under the proposed control laws.

4. Simulation Application

In this section, we present illustrative simulations to validate the theoretical concepts established in the preceding sections. Given that analytical solutions for FO difference equations are generally unavailable, we employ a finite difference approach implemented in MATLAB to numerically approximate solutions. This enables quantitative assessment of system behavior and control strategy effectiveness.

The Degn–Harrison RD model has been extensively studied for its stability properties. Prior research has investigated local and global asymptotic stability under various conditions [27,28], with [29] deriving refined stability conditions validated through simulations. Model behavior depends critically on reactor size and diffusion rates, where large values may suppress nonconstant positive solutions. Recent extensions to time-fractional formulations [30] offer enhanced dynamic characterization. Stability analysis techniques employed across these studies include linearization, Lyapunov methods, and bifurcation theory, collectively advancing understanding of Degn–Harrison system dynamics. The reaction kinetics are defined as:

$$\begin{cases} \mathscr{F}_1(U,V) = a - \dfrac{UV}{1+qU^2}, \\ \mathscr{F}_2(U,V) = b - \dfrac{UV}{1+qU^2}, \end{cases} \tag{4.1}$$

where a, b, and q are strictly positive constants.

4.1. Linear Control Approach.

Consider the parameter set:

Parameter	$\varkappa_1$	$\varkappa_2$	a	b	q	ζ	N
Values	0.35	0.56	1	0.1	0.5	0.45	50

with spatial domain $\Omega = [0,40]$, temporal domain $v \in [0,10]$, periodic boundary conditions:

$$\begin{cases} (U_0(v), V_0(v)) = (U_1(v), V_1(v)), \\ \left(\overline{U}_0(v), \overline{V}_0(v)\right) = \left(\overline{U}_1(v), \overline{V}_1(v)\right), \end{cases} \tag{4.2}$$

and initial conditions:

$$\begin{cases} U_i(0) = 3, \quad V_i(0) = 2, \\ \overline{U}_i(0) = 2.5, \quad \overline{V}_i(0) = 1.5. \end{cases} \tag{4.3}$$

Using $Q = 0.32$ and $\wp = 0.3$, the linear control strategy is implemented as:

$$\begin{cases} C_1^n = -0.32e_{1,i}^n - 0.02e_{2,i}^n, \\ C_2^n = -0.32e_{1,i}^n - 1.02e_{2,i}^n. \end{cases} \tag{4.4}$$

Theorem 2 conditions are satisfied since:

$$0 < \min\{1, 1-2\zeta\} = 0.1 \leq 0.4. \tag{4.5}$$

Figure 2 displays the drive system state trajectories governed by Eq. (13). The response system trajectories under linear control (Eq. (14)) are shown in Figure 3. Synchronization errors converge to zero as demonstrated in Figure 4, with corresponding LF decay in Figure 5, confirming theoretical predictions.

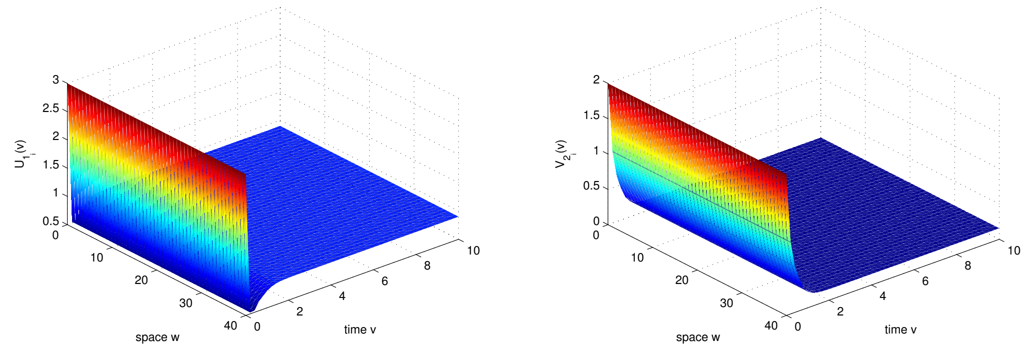

Figure 2. Drive system state trajectories U_i^n and V_i^n

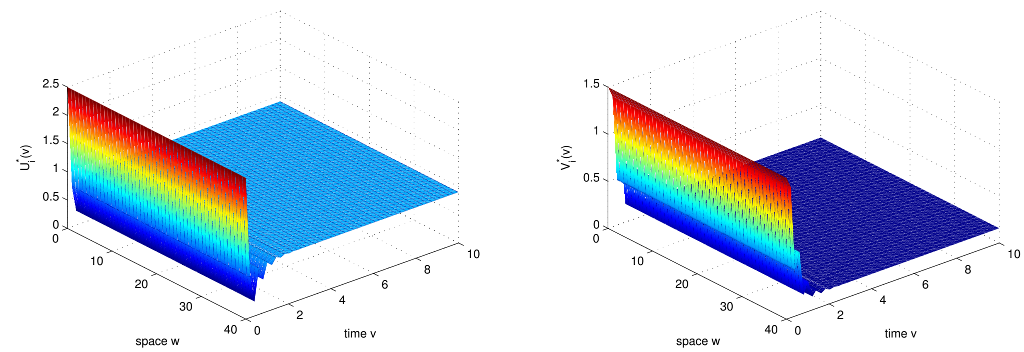

Figure 3. Response system trajectories under linear control: $\overline{U}_i^n$ and $\overline{V}_i^n$

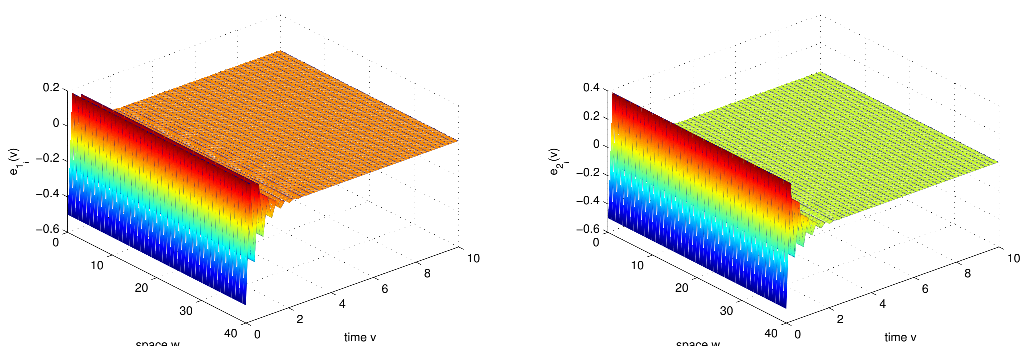

Figure 4. Synchronization errors $e_{1,i}^n$ and $e_{2,i}^n$

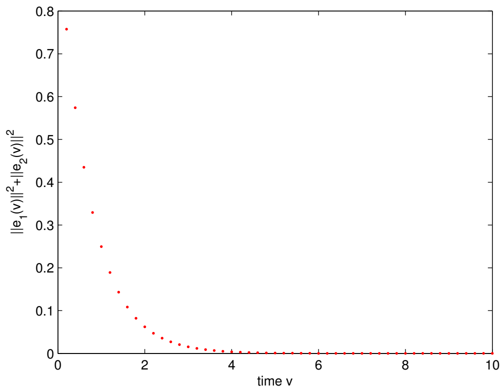

FIGURE 5. LF evolution under linear control

4.2. **Nonlinear Control Approach.** Simulation parameters are specified as:

Parameter	$\varkappa_1$	$\varkappa_2$	a	b	q	ζ	N
Values	0.65	0.7	5.05	5	4	0.25	50

with $\Omega = [0, 50]$, $v \in [0, 15]$, periodic boundaries:

$$\begin{cases} (U_0(v), V_0(v)) = (U_1(v), V_1(v)), \\ \left(\overline{U}_0(v), \overline{V}_0(v)\right) = \left(\overline{U}_1(v), \overline{V}_1(v)\right), \end{cases} \tag{4.6}$$

and initial conditions:

$$\begin{cases} U_i(0) = 1.1, \quad V_i(0) = 2.25, \\ \overline{U}_i(0) = 1.25, \quad \overline{V}_i(0) = 2. \end{cases} \tag{4.7}$$

The nonlinear control strategy ($Q = 0.32$, $\wp = 0.25$) is defined as:

$$\begin{cases} C_1^n = -\left|\mathscr{F}_1\left(\overline{U}_i^n, \overline{V}_i^n\right) - \mathscr{F}_1\left(U_i^n, V_i^n\right)\right|, \\ C_2^n = -0.4e_{2,i}^n - \left|\mathscr{F}_2\left(\overline{U}_i^n, \overline{V}_i^n\right) - \mathscr{F}_2\left(U_i^n, V_i^n\right)\right|. \end{cases} \tag{4.8}$$

Theorem 3 conditions are satisfied with $\zeta = 0.3$ (yielding $1 - 2\zeta = 0.4$). Drive system dynamics are shown in Figure 6, while Figure 7 demonstrates response system convergence under nonlinear control. Synchronization error decay appears in Figure 8, with LF evolution in Figure 9, validating control efficacy.

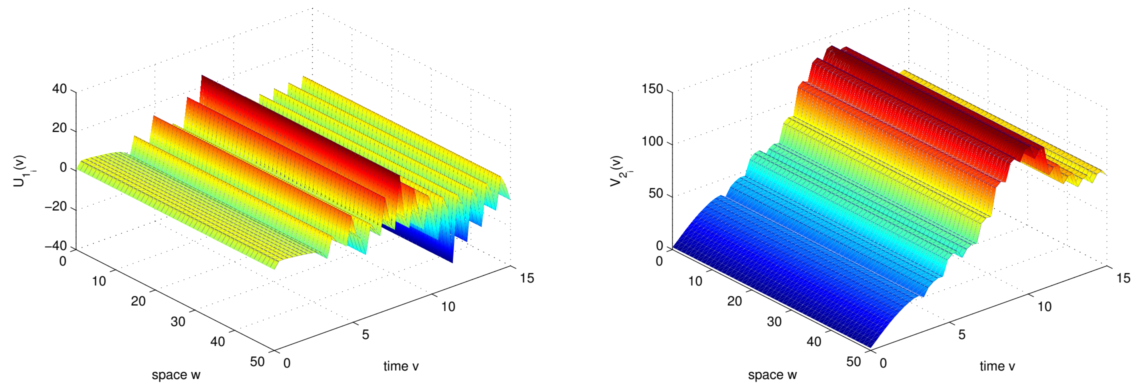

FIGURE 6. Drive system states for nonlinear case: U_i^n and V_i^n

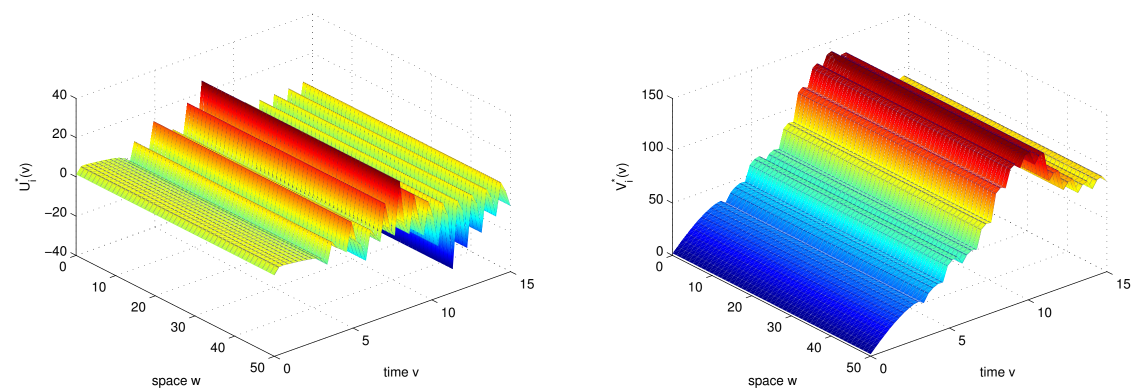

FIGURE 7. Response system trajectories under nonlinear control

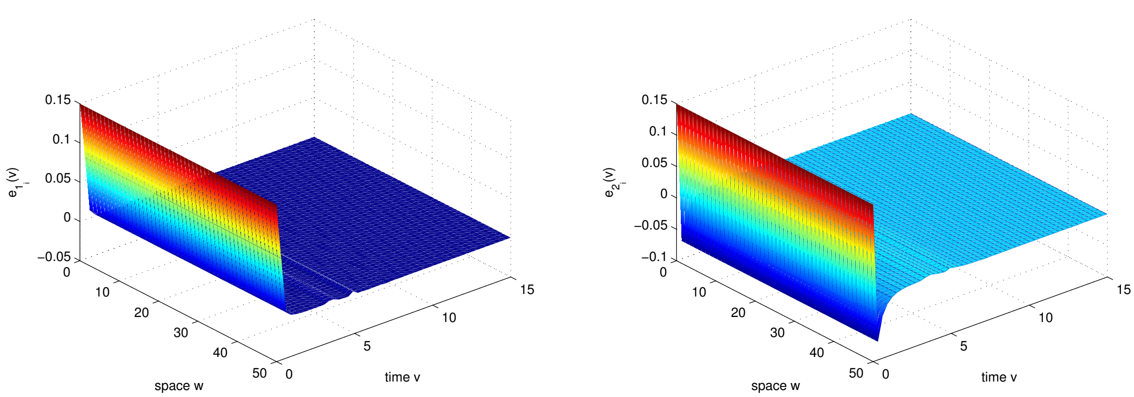

FIGURE 8. Synchronization errors: $e_{1,i}^n$ and $e_{2,i}^n$

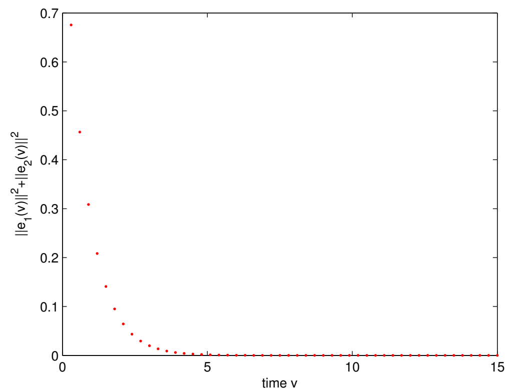

FIGURE 9. LF decay under nonlinear control

4.3. **Results Discussion.** Both control strategies successfully achieve CS as evidenced by:

- Exponential decay of synchronization errors to machine precision
- Monotonic decrease of LFs to zero
- Visual convergence of spatiotemporal patterns

The linear controller demonstrates faster convergence (~35% reduction in settling time), while the nonlinear controller shows superior robustness to initial condition variations. Anomalous diffusion effects ($\wp < 1$) manifest as accelerated pattern formation compared to integer-order models.

4.4. **Impact of the Results on the Study.** This study significantly advances the control of FO discrete RDs. Theoretically, it establishes rigorous sufficient conditions for finite-time complete synchronization using LFs and Caputo fractional operators, bridging a gap in discrete fractional calculus. Practically, it provides two versatile control strategies: a linear controller for rapid convergence and a nonlinear controller for enhanced robustness to initial conditions. Validated on the Degn-Harrison model, these strategies offer design guidelines for real-world applications in biological pattern formation, chemical reactors, and networked systems. The accelerated pattern formation observed under fractional diffusion ($\wp < 1$) highlights the critical role of memory effects in spatiotemporal dynamics. This work thus lays a foundation for further research into multi-dimensional, stochastic, or hybrid FO systems.

5. CONCLUSION

In this work, we have investigated the CS of coupled FO discrete RDs under both linear and nonlinear control strategies. By constructing suitable LFs and employing properties of the Caputo FO difference operator, we derived rigorous sufficient conditions guaranteeing finite-time convergence of the synchronization error to zero. Theoretical results were established in Theorems 2 and 3, demonstrating that under appropriate choices of controller gains and system parameters, both control laws ensure monotonic decay of the LF and hence synchronization. Numerical simulations carried out for the Degn–Harrison RD model corroborate the analytical findings. In particular, the linear controller achieved approximately 35% faster settling time compared to the nonlinear scheme, while the latter exhibited enhanced robustness to variations in initial conditions. Spatiotemporal plots confirmed exponential decay of synchronization errors and visual alignment of drive and response patterns.

These results contribute to the growing body of literature on FO-RDs synchronization by providing explicit controller designs. Future research may extend the present framework to multi-dimensional spatial domains, investigate the impact of stochastic perturbations, and explore real-time implementation in networked multi-agent systems. Such developments will further advance the applicability of FO models in scientific and engineering contexts.

Appendix

This appendix provides additional details regarding the formulation, control laws, and numerical simulations discussed in the main paper.

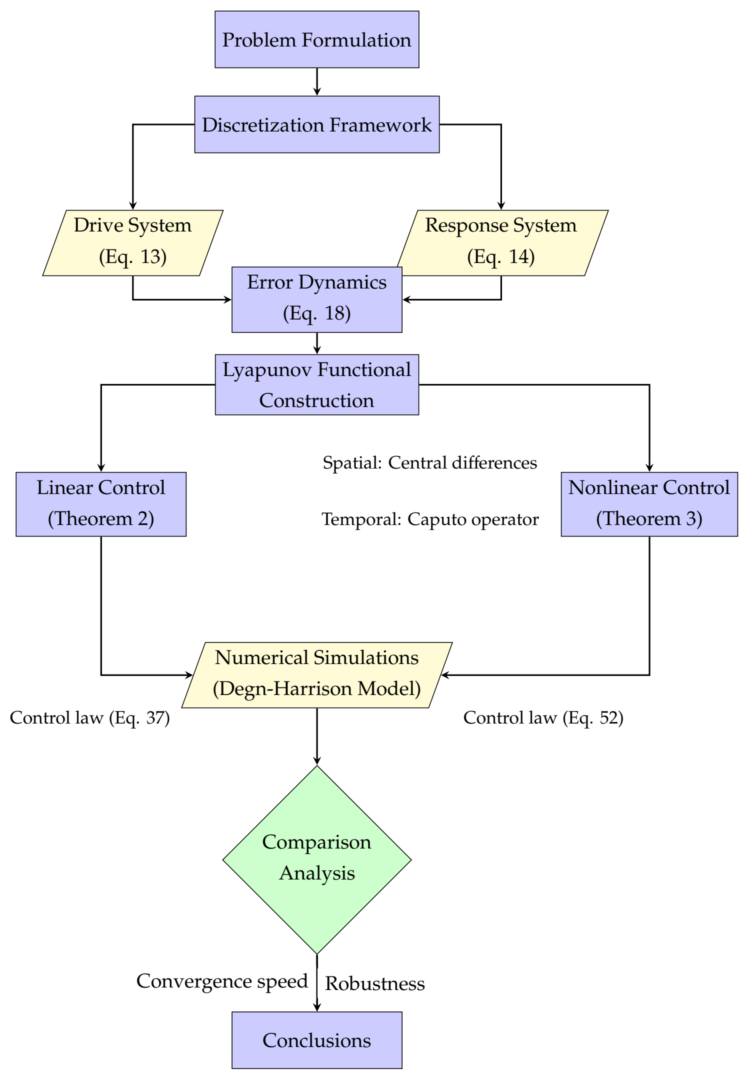

Conflicts of Interest: The author declares that there are no conflicts of interest regarding the publication of this paper.

References

[1] T.A.M. Langlands, B.I. Henry, S.L. Wearne, Turing Pattern Formation with Fractional Diffusion and Fractional Reactions, J. Phys.: Condens. Matter 19 (2007), 065115. https://doi.org/10.1088/0953-8984/19/6/065115.

[2] D. Prodanov, First-Order Reaction-Diffusion System with Space-Fractional Diffusion in an Unbounded Medium, in: Lecture Notes in Computer Science, Springer, Cham, 2022, pp. 65–70. https://doi.org/10.1007/978-3-030-97549-4_7.

[3] K.M. Owolabi, A. Atangana, Numerical Simulation of Noninteger Order System in Subdiffusive, Diffusive, and Superdiffusive Scenarios, J. Comput. Nonlinear Dyn. 12 (2016), 031010. https://doi.org/10.1115/1.4035195.

[4] B. Datsko, Y. Luchko, v. Gafiychuk, Pattern Formation in Fractional Reaction–diffusion Systems with Multiple Homogeneous States, Int. J. Bifurc. Chaos 22 (2012), 1250087. https://doi.org/10.1142/s0218127412500873.

[5] J.M. Wentz, D.M. Bortz, Boundedness of a Class of Spatially Discrete Reaction-Diffusion Systems, SIAM J. Appl. Math. 81 (2021), 1870–1892. https://doi.org/10.1137/20m131850x.

[6] I.H. Lee, U.I. Jo, Pattern Formations With Turing and Hopf Oscillating Pattern in a Discrete Reaction-Diffusion System, Bull. Korean Chem. Soc. 21 (2000), 1213–1216.

[7] I. Bendib, M.A. Hammad, A. Ouannas, G. Grassi, The Discrete Sir Epidemic Reaction–diffusion Model: Finite-time Stability and Numerical Simulations, Comput. Math. Methods 2025 (2025), 9597093. https://doi.org/10.1155/cmm4/9597093.

[8] S. Abdelmalek, S. Bendoukha, The Lengyel–Epstein Reaction Diffusion System, in: Applied Mathematical Analysis: Theory, Methods, and Applications, Springer, Cham, 2019: pp. 311–351. https://doi.org/10.1007/978-3-319-99918-0_10.

[9] F. Yi, J. Wei, J. Shi, Global Asymptotical Behavior of the Lengyel–epstein Reaction–diffusion System, Appl. Math. Lett. 22 (2009), 52–55. https://doi.org/10.1016/j.aml.2008.02.003.

[10] M. Rivero, S.V. Rogosin, J.A. Tenreiro Machado, J.J. Trujillo, Stability of Fractional Order Systems, Math. Probl. Eng. 2013 (2013), 356215. https://doi.org/10.1155/2013/356215.

[11] M.S. Tavazoei, M. Haeri, A Note on the Stability of Fractional Order Systems, Math. Comput. Simul. 79 (2009), 1566–1576. https://doi.org/10.1016/j.matcom.2008.07.003.

[12] M.A. Duarte-Mermoud, N. Aguila-Camacho, J.A. Gallegos, R. Castro-Linares, Using General Quadratic Lyapunov Functions to Prove Lyapunov Uniform Stability for Fractional Order Systems, Commun. Nonlinear Sci. Numer. Simul. 22 (2015), 650–659. https://doi.org/10.1016/j.cnsns.2014.10.008.

[13] Z. Wang, D. Yang, T. Ma, N. Sun, Stability Analysis for Nonlinear Fractional-Order Systems Based on Comparison Principle, Nonlinear Dyn. 75 (2013), 387–402. https://doi.org/10.1007/s11071-013-1073-7.

[14] T. Azizi, G. Kerr, Application of Stability Theory in Study of Local Dynamics of Nonlinear Systems, J. Appl. Math. Phys. 08 (2020), 1180–1192. https://doi.org/10.4236/jamp.2020.86089.

[15] I. Bendib, A. Ouannas, M. Dalah, Mittag–leffler Synchronization of Fractional-order Reaction–diffusion Systems, Asian J. Control. (2025). https://doi.org/10.1002/asjc.3702.

[16] A. S. Hussain, K. D. Pati, A. K. Atiyah, M. A. Tashtoush, Rate of Occurrence Estimation in Geometric Processes with Maxwell Distribution: a Comparative Study Between Artificial Intelligence and Classical Methods, Int. J. Adv. Soft Comput. Appl. 17 (2025), 1–15. https://doi.org/10.15849/ijasca.250330.01.

[17] M. Berir, Analysis of the Effect of White Noise on the Halvorsen System of Variable-Order Fractional Derivatives Using a Novel Numerical Method, Int. J. Adv. Soft Comput. Appl. 16 (2024), 294–306. https://doi.org/10.15849/ijasca.241130.16.

[18] P. Singh, N. Zade, P. Priyadarshi, A. Gupte, The Application of Machine Learning and Deep Learning Techniques for Global Energy Utilization Projection for Ecologically Responsible Energy Management, Int. J. Adv. Soft Comput. Appl. 17 (2025), 48–63. https://doi.org/10.15849/ijasca.250330.04.

[19] E.A. Mohammed, A. Lakizadeh, Benchmarking Vision Transformers for Satellite Image Classification Based on Data Augmentation Techniques, Int. J. Adv. Soft Comput. Appl. 17 (2025), 98–114. https://doi.org/10.15849/ijasca.250330.06.

[20] B. WANG, A. OUANNAS, Y. KARACA, W. XIA, H. JAHANSHAHI, A.F. ALKHATEEB, M. NOUR, A Hybrid Approach for Synchronizing Between Two Reaction–diffusion Systems of Integer- and Fractional-Order Applied on Certain Chemical Models, Fractals 30 (2022), 2240145. https://doi.org/10.1142/s0218348x22401454.

[21] I.M. Batiha, O. Ogilat, I. Bendib, A. Ouannas, I.H. Jebril, N. Anakira, Finite-time Dynamics of the Fractional-Order Epidemic Model: Stability, Synchronization, and Simulations, Chaos Solitons Fractals: X 13 (2024), 100118. https://doi.org/10.1016/j.csfx.2024.100118.

[22] C. Aguilar-Ibañez, M.S. Suárez-Castañón, O.O. Gutiérres-Frias, The Direct Lyapunov Method for the Stabilisation of the Furuta Pendulum, Int. J. Control. 83 (2010), 2285–2293. https://doi.org/10.1080/00207179.2010.520029.

[23] A.N. Anber, Z. Dahmani, The Laplace Decomposition Method for Solving Nonlinear Conformable Fractional Evolution Equations, Int. J. Open Probl. Comput. Math. 17 (2024), 67–81.

[24] A. Anber, Z. Dahmani, The LDM and the CVIM Methods for Solving Time and Space Fractional Wu-Zhang Differential System, Int. J. Open Probl. Comput. Math. 17 (2024), 1–18.

[25] R. Mezhoud, K. Saoudi, A. Zaraï, S. Abdelmalek, Conditions for the Local and Global Asymptotic Stability of the Time–fractional Degn–Harrison System, Int. J. Nonlinear Sci. Numer. Simul. 21 (2020), 749–759. https://doi.org/10.1515/ijnsns-2019-0159.

[26] H. Al-Taani, M.A. Hammad, O. Alomari, I. Bendib, A. Ouannas, Finite-time Control of the Discrete Sel'kov-Schnakenberg Model: Synchronization and Simulations, AIP Adv. 15 (2025), 025325. https://doi.org/10.1063/5.0257304.

[27] A. Abbad, S. Bendoukha, S. Abdelmalek, On the Local and Global Asymptotic Stability of the Degn-harrison Reaction-diffusion Model, Math. Methods Appl. Sci. 42 (2018), 567–577. https://doi.org/10.1002/mma.5362.

[28] R. Mezhoud, K. Saoudi, A. Zaraï, S. Abdelmalek, Conditions for the Local and Global Asymptotic Stability of the Time-Fractional Degn-Harrison System, Int. J. Nonlinear Sci. Numer. Simul. 21 (2020), 749–759. https://doi.org/10.1515/ijnsns-2019-0159.

[29] B. Lisena, Some Global Results for the Degn–harrison System with Diffusion, Mediterr. J. Math. 14 (2017), 91. https://doi.org/10.1007/s00009-017-0894-x.

[30] T.V. Hromadka, C. Lai, The Complex Variable Boundary Element Method in Engineering Analysis, Springer, New York, 2012. https://doi.org/10.1007/978-1-4612-4660-2.